Fixed-wing approach techniques for complex environments

P. R. Thomas
p.thomas@bristol.ac.uk
S. Bullock, U. Bhandari and T. S. Richardson
Department of Aerospace Engineering
University of Bristol
Bristol
UK

ABSTRACT

The landing approach for fixed-wing small unmanned air vehicles (SUAVs) in complex environments such as urban canyons, wooded areas, or any other obscured terrain is challenging due to the limited distance available for conventional glide slope descents. Alternative approach methods, such as deep stall and spin techniques, are beneficial for such environments but are less conventional and would benefit from further qualitative and quantitative understanding to improve their implementation. Flight tests of such techniques, with a representative remotely piloted vehicle, have been carried out for this purpose and the results are presented in this paper. Trajectories and flight data for a range of approach techniques are presented and conclusions are drawn as to the potential benefits and issues of using such techniques for SUAV landings. In particular, the stability of the vehicle on entry to a deep stall was noticeably improved through the use of symmetric inboard flaps (crow brakes). Spiral descent profiles investigated, including spin descents, produced faster descent rates and further reduced landing space requirements. However, sufficient control authority was maintainable in a spiral stall descent, whereas it was compromised in a full spin.

Paper No. 4109. Manuscript received 4 Decenber 2013, revised version received 7 November 2014, accepted 27 March 2015.

https://doi.org/10.1017/S0001924000004292 Published online by Cambridge University Press

NOMENCLATURE

α	angle-of-attack
β	angle of sideslip
γ	flight path angle
φ, θ, ψ	roll, pitch, yaw angles
p, q, r	roll, pitch, yaw rates
V	airspeed
x, y, z	position from launch
$\dot{z}$	descent speed
h	height
l	horizontal landing distance
τ	throttle input
η, ξ, ζ	elevator, aileron, and rudder inputs
δ_f	inboard flap input
$(\cdot)_e$	trim value

1.0 INTRODUCTION

Small unmanned air vehicles (SUAV), sometimes referred to as miniature UAVs, are remotely operated aircraft that are portable enough to be carried by a single person. They range in size from a few centimetres to a few metres, a classification above micro air vehicles (see Fig. 1). The UK Civil Aviation Authority has defined 'small' unmanned aircraft as 'having a mass of not more than 20kg without its fuel but including any articles or equipment'[1]. SUAVs are widely used in military ground-based ISR (intelligence, surveillance, and reconnaissance) tasks whilst civil applications are increasingly being investigated. Such uses could include disaster assessment, antidrug reconnaissance platforms, aerial photography and mapping, and various other low-payload tasks that benefit from a quickly deployable aerial platform. A key benefit of SUAVs is the flexibility to deploy them without the need for conventional resources or runways. Consequently they are of significant use in complex environments such as urban canyons, wooded areas or otherwise restricted terrain. However, the subsequent landing and recovery of the aircraft in such terrain is

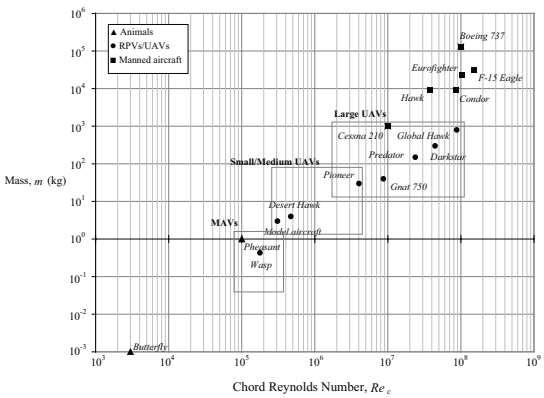


Figure 1. Classification of various aircraft.

https://doi.org/10.1017/S0001924000004292 Published online by Cambridge University Press

more complicated; conventional approach glide slopes and brake-to-stop landings are severely restricted due to the lack of unobstructed airspace, landing strip length, or suitable terrain for landing and braking. Alternative approaches therefore need to be considered and developed.

1.1 Deep stalling

An aircraft stall, where flow separation is sufficient to lead to a reduction in lift with increasing angle-of-attack, is effective at quickly reducing the lift generated by the wing, and thus reducing altitude. A stall approach takes advantage of this loss in altitude but in a controlled fashion in order to bring the vehicle down on a larger descent gradient. Above the critical stall angle-of-attack, if the pitching moments can be balanced the lift and drag forces can also be stabilised. By taking advantage of the large drag force, the horizontal speed of the vehicle can be effectively reduced and brought down on a steep and consistent glide slope[2].

The balancing of pitching moments is necessary for control of the airspeed and glide slope. In a conventional configuration the means to do this is by either the thruster or the elevator. This

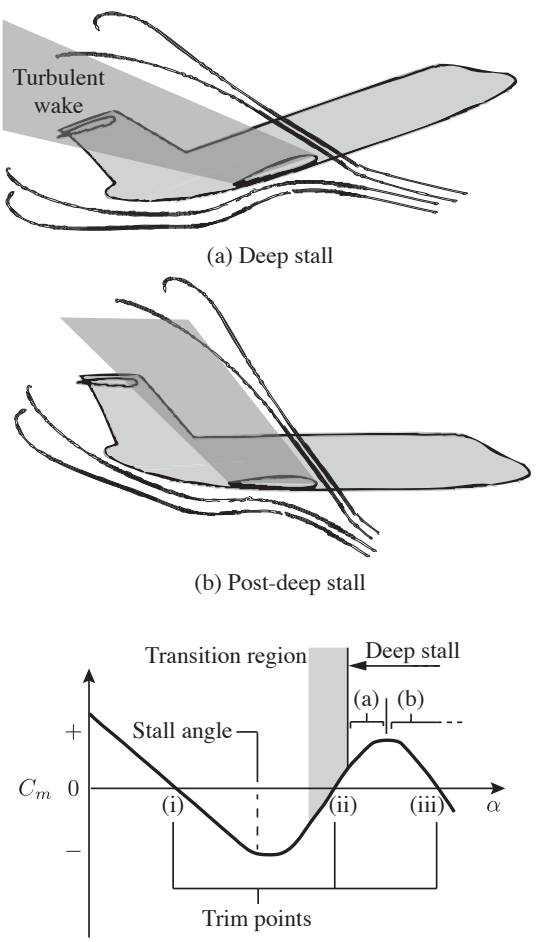


Figure 2. Deep stall of a T-tail configuration. The three trim points correspond to normal flight (stable), during stall (unstable), and in deep stall (stable).

https://doi.org/10.1017/S0001924000004292 Published online by Cambridge University Press

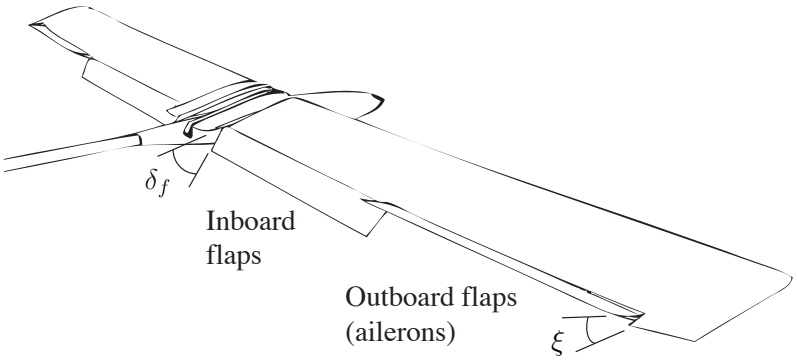


Figure 3. Crow braking.

means that, unlike the main wing, the airflow over the elevator (and its preceding tailplane) must be predominantly attached. A stall landing at a high angle-of-attack is sometimes called a deep stall landing[2,3], though 'deep-stall' specifically refers to the highly uncontrollable post-stall condition where pitch authority is significantly reduced. It was studied through both experimental wind-tunnel testing[4] and simulator studies[5,6] back in 1965 at NASA. It is a common problem for T-tail configurations where the turbulent wake from the stalled main wing blankets the tailplane and elevator, making pitch control inert. It can also be encountered in certain situations on other aircraft configurations with a rearwards centre of mass, and on canard configurations where the aft wing stalls, forcing the aircraft to pitch up and push the canard into stall[7]. A similar process between an F-16's wing and strakes would lead it to deep stall between 50 and 60°degrees angle-of-attack[8]

Figure 2 illustrates that in a stall the aircraft becomes longitudinally unstable (where the gradient of the C_m–α plot becomes positive). As the angle-of-attack increases aircraft of a susceptible configuration will transition to a deep stall as the tailplane is engulfed in the low-energy wake from the wing. However as the angle-of-attack increases further, the tailplane may emerge from the wake (Fig. 2(b)) and longitudinal stability may be restored. The aircraft can now be balanced in a stable, deep stall condition at a high angle-of-attack (trim point (iii) in Fig. 2). However, as it would need to pitch down to the extent that the tailplane is forced back through the low energy wake, the aircraft may not be able to recover from this stalled condition. Whilst a serious problem for conventional airliners, alternative methods of pitch control such as thrust vectoring on super-manoeuvrable aircraft can make deep stalls more recoverable. A variable-pitch tailplane (stabilator) has been used to reduce the local angle-of-attack of a tailplane to provide pitch authority during a deep stall[9].

Deep stall approach and landing features prominently in the techniques of biomimetic UAVs[10,11]. However, whilst the process of stall approach employs drag to reduce the airspeed, a 'perching manoeuvre' primarily reduces the airspeed through orientating the lift vector. In addition to landing in confined spaces, the avian-inspired landing mechanisms could allow vehicles to re-launch themselves using stored potential energy, eliminating manual recovery and increasing system autonomy. A large, fast pitch-up manoeuvre is typically sufficient to initiate a dynamic stall of most vehicle configurations necessary for a deep stall. This is normally followed by a brief increase in lift due to the shedding of leading edge vortices temporarily energising the flow, enabling it to stay attached to the surface beyond the quasi-static stall angle. After the stall delay, the vortex quickly detaches and the accompanying reduction in lift and pitching moment from stall occurs. At the

https://doi.org/10.1017/S0001924000004292 Published online by Cambridge University Press

start, and for the duration of the stalled descent, the separated flow across the vehicle's wing will decay into highly unsteady wing vortices which are expected to be the cause of often experienced wing rock[12]. The unsteadiness peaks at the start of the stall, where a quick progression through it is advisable in order to avoid any asymmetry developing which can push the stall into a spin[9].

As the descent is steeper, and therefore faster, additional protection on landing may be required to protect the airframe structure and payload. This could be provided in the form of deployable parachutes or inflatable sleeves. A more elaborate landing manoeuvre involves inverting the vehicle to present a better landing surface, a method which is used on a number of currently deployed SUAVs.

1.2 Crow braking

Crow Braking (CB) is a technique mainly used on gliders without dedicated air brakes in order to rapidly reduce airspeed for landing. In a CB manoeuvre the main wing's inboard flaps are deflected downwards to their maximum travel whilst both ailerons are deflected symmetrically upwards, shown in Fig. 3. With full-span flaps, vortices formed between the control surfaces create extra vortex drag in addition to the form drag from the deflected flaps and ailerons. Crow braking is effective in the absence of dedicated air brakes, however a nose pitch-up may be produced which needs to be countered with the elevator in order to prevent the aircraft from stalling[13].

1.2.1 Spin

Auto-rotation of an aircraft about its spin axis is a result of differential drag between the port and starboard wings as a result of one of them being in a deeper stall than the other. This differential drag causes the aircraft to yaw towards the deeper stalled wing causing the aircraft to spin on a downward corkscrew trajectory. A spin can be deliberately initiated by applying a yawing motion whilst stalling the aircraft. The resulting moment, coupled with the unsteady flow, is typically all that is necessary to start the spin. Such an unbalanced aircraft during a stall is the primary cause for unintentional spinning. Standard procedures exists which, when applied, are capable of recovering an aircraft from spin. The suitability of intentionally entering a spin to bleed altitude is therefore dependent on the ease and repeatability at which the specific aircraft in question can escape it.

Due to the catastrophic results from an uncontrolled spin, and the uncertain reliability of successful recovery, its use as a method of controlled descent has been mostly avoided outside the interests of model plane enthusiasts. Deliberately entering spin would allow the aircraft to rapidly descend in a relatively small column of air, suggesting that a controlled execution has the potential to yield high positional precision in restricted environments with very small airspace. Whilst a spiral dive, which differs from a spin in that the aircraft is not stalled, would achieve the same effect the aircraft would have to contend with a similar set of problems involving managing the fast descent rate and ensuring sufficient altitude to safely exit the dive.

1.2.2 Thrust vectoring and reversal

Reducing thrust on the approach is the most direct way to decrease altitude. A controllable pitch propeller could be used to reduce and, just prior to landing, reverse the direction of thrust thereby producing a braking effect and land on a smaller landing strip. In contrast, thrust vectoring enables rotation of the direction of thrust, enabling further augmentation in directional control of the aircraft. Vectored thrust has successfully been used to incorporate vertical take-off and landing (VTOL) capabilities and provide pitch control in a variety of (manned and unmanned) fixed wing aircraft. Thrust vectoring and reversal have the potential to produce a faster descent compared

https://doi.org/10.1017/S0001924000004292 Published online by Cambridge University Press

to thrust reduction alone, offering the potential of landing using much smaller landing strips[10]. Successful implementation will depend greatly on the dynamic effects on the vehicle's stability and in successfully balancing the moments on the aircraft when the thrust is significantly altered or reversed.

1.3 Research goals

In order to develop qualitative and quantitative understanding a series of flight tests were carried out employing some of the approach methods discussed above. By collecting flight data on a variety of approach techniques accurate flight dynamic models can be developed in the future. The techniques of interest in this paper have been limited to the first three methods discussed: deep stall, crow braking, and spin descents.

This paper is organised as follows Section 2 details the flight vehicle and data logging hardware used. In Section 3 a description of each flight manoeuvre is presented and preliminary flight data illustrated. A comparison and discussion of the methods from analysis of the flight test results then proceeds in Section 4, followed by the conclusions of this work.

2.0 RESEARCH PLATFORM

In order to compare the approach techniques, comparable flight data from a single test-bed aircraft was desirable. Commercial off-the-shelf components were used in order to minimise cost and permit straightforward repair or replacement of parts. This included the vehicle, which was based on a HobbyKing Eagle (Fig. 4). It was selected as it is similar in size, mass, and configuration to typical SUAVs employing a high wing, a push propeller, and forward payload bay. It is constructed from fibreglass and ply wood and has a wingspan of just under 1·7m. Entry into deep stall with the Eagle was initially problematic, with it producing consistent uncontrollable wing drop. A likely explanation for this was asymmetric stall caused by insufficient elevator control authority, such that the angle-of-attack attained was only producing marginal stall conditions. Additionally, the wing loading required a high velocity for straight-and-level flight and the initial entry into the stall did not provide a rapid enough reduction in velocity. A lower-than expected control authority available in these conditions made it difficult to initiate a deep stall. Several modifications to the



Figure 4. The Eagle deep stall test vehicle.

https://doi.org/10.1017/S0001924000004292 Published online by Cambridge University Press

base airframe were made to improve on these limitations:

- Increase in elevator size and travel to provide sufficient authority to achieve high incidence
- Increase in rudder size and travel to provide increased authority to maintain control within the stall
- Addition of inboard split flaps to perform crow braking
- A new speed controller, motor and propeller, and a reinforced motor mounting plate, to increase robustness against rapid changes in thrust demand (the stock speed controller failed under rapid demand changes)
- Relocation of the centre of mass rearwards to promote easier entry into deep stall

The Eagle was fitted with a MicroPilot MP2128g autopilot system with sensor suite, shown in Fig. 5. The autopilot functionality was disabled and instead used solely as a data-logger to record:

- linear accelerations, a_x, a_y, a_z
- angular rates, *p, q, r*
- attitude angles, φ, θ, ψ
- GPS position, speed, and altitude
- pressure altitude, *h*
- pilot control inputs, τ, η, ξ

Additionally, angle-of-attack, α, was logged via an analog-to-digital converter measuring output from a low-friction hall-effect encoder fitted with a vane, shown in Fig. 6. Airspeed. *V*, was measured via differential pressure between a static port and pitot tube. The location of both these instruments on the airframe was a compromise between increasing survivability upon landing and access to the freestream flow. The upwash effect on the angle-of-attack measurements was not investigated in great detail, and is expected to introduce some error in the quantified results, but not the overall trends.

The pilot control inputs from the RC receiver, except for the rudder and inboard flaps, were logged by passing the receiver signals to the servos and data-logger simultaneously. Since the actual control surfaces were not measured directly, there is an assumption that the control surfaces responded accurately to the control demands. The latency between demands and control surface deflections has also been neglected, which is not too unreasonable given the high-speed servos used (1·6ms/deg unloaded). Furthermore, the interest in measuring the control surfaces was primarily to obtain the magnitude of deflection and the time it occurred, rather than capture the higher order dynamics of the control input system. The limited payload capacity of the SUAV prevented the use of a radio modem for telemetry download. The data logs were recovered after flight instead, which provided higher-frequency and higher-resolution data compared to the radio modem system.

3.0 FLIGHT TESTS

After pilot familiarisation and equipment testing, several flights of each descent type described below were conducted. A typical test flight is shown in Fig. 7, where three to four manoeuvres were performed within a single flight in order to manage the vehicle's power supply (needed for both motor and datalogger) and to ensure manageable flight log sizes when downloaded from the datalogger. Each approach was exited in the region of 20 metres before reaching the ground as a buffer to unintended landings and potential damage to equipment. Actual landings at the end of each flight were by the conventional approach.

https://doi.org/10.1017/S0001924000004292 Published online by Cambridge University Press

3.1 Conventional approach (for skid landing)

Approaches with conventional glide slopes were performed for comparison with the other descent modes. On the approach the throttle was reduced and the elevator used to control the airspeed to maintain the glide slope. Just prior to landing the throttle was shut-off and a landing flare is performed.

The descent rate was around $2ms^{-1}$ for most of the descents whilst the airspeed averaged at about $18ms^{-1}$ with a measured angle-of-attack of around 2°. Pitch angle θ varied between 0 and −10°, averaging around −9°. From these values the flight path angle γ can be approximated as $\gamma \approx \theta - \alpha$; −11° in this case. On actual landings a flare just prior to touchdown brought the incidence up briefly to approximately 8°. Using a combination of throttle reduction and full upwards elevator deflection, the aircraft was commanded to rapidly pitch up, bringing the aircraft to a measured incidence of around 30° and into a stable stall, producing a loss of lift and increase in drag. This produced a steady descent with a low lift-to-drag ratio. Although it was possible to conduct a slow transition into the deep stall the transient and asymmetric effects on the vehicle shortly after stall were difficult to control. When attempted, without reactive input from the pilot the aircraft was subject to roll and yaw divergence and typically began to spin. Consequently rapid entry into the deep stall was performed. The rudder, and to some extent the ailerons, were used to maintain descent in a straight line.

3.2 Deep stall

Using a combination of throttle reduction and full upwards elevator deflection, the aircraft was commanded to rapidly pitch up, bringing the aircraft to a measured incidence of around 30° and into a stable stall, producing a loss of lift and increase in drag. This produced a steady descent with a low lift-to-drag ratio. Although it was possible to conduct a slow transition into the deep stall the transient and asymmetric eects on the vehicle shortly after stall were dicult to control. When attempted, without reactive input from the pilot the aircraft was subject to roll and yaw divergence and typically began to spin. Consequently rapid entry into the deep stall was performed. The rudder, and to some extent the ailerons, were used to maintain descent in a straight line.

In order to enter the stall the pilot rapidly reduced the throttle to around 20% whilst stepping the elevator up. Upon reducing the throttle, the pitch-down moment generated by the high motor arrangement is reduced causing an upwards pitch. At this incidence the wing was suciently stalled, resulting in reduced lift and increased drag with a subsequent reduction in airspeed. A steady descent was achieved, with a rate averaging $5{\cdot}8ms^{-1}$ and a flight path angle in the region of –30°.

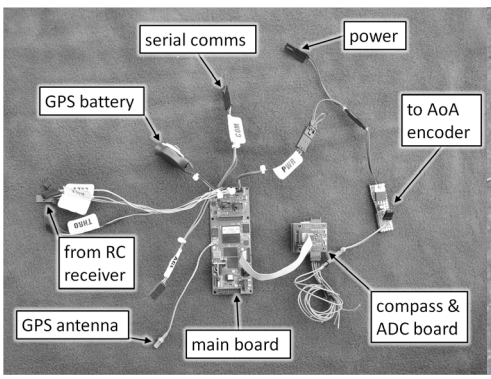


Figure 5. Instrumentation and datalogger.

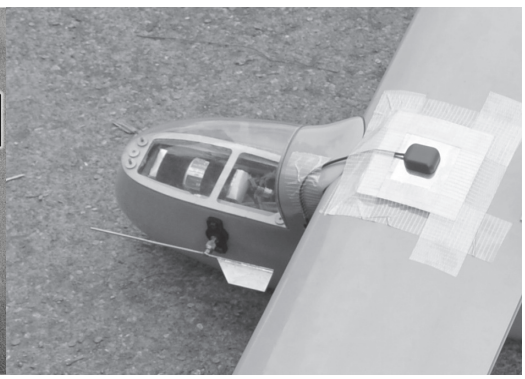


Figure 6. Angle-of-attack vane, with GPS antenna shown.

https://doi.org/10.1017/S0001924000004292 Published online by Cambridge University Press

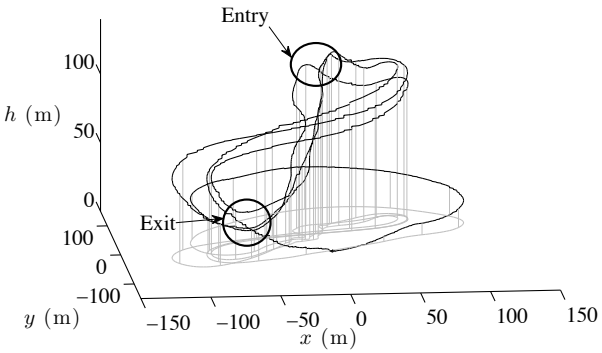


Figure 7. Typical deep stall test flight.

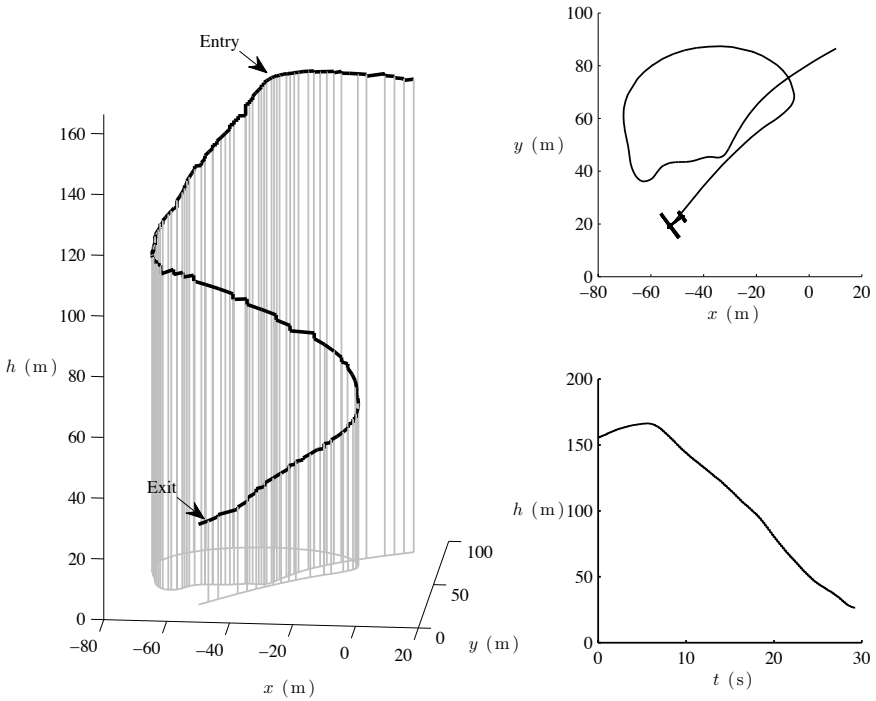


Figure 8. A spiral deep stall descent.

3.3 Spiral deep stall

Entry into a deep stall followed the same process as before, but the descent was also made in a controlled spiral. A small rudder input was applied to promote the turn; as a result the inside wing drops and opposite aileron was required to stabilise the bank angle at around 15–20 degrees. The higher drag on the inside wing further increases the turn rate, with the turn continuing until rudder deflection was removed.

In this landing manoeuvre the aircraft tended to depart in both roll and yaw, in a greater magnitude than in a straight deep stall resulting in high pilot workload in the lateral and longitudinal directions.

https://doi.org/10.1017/S0001924000004292 Published online by Cambridge University Press

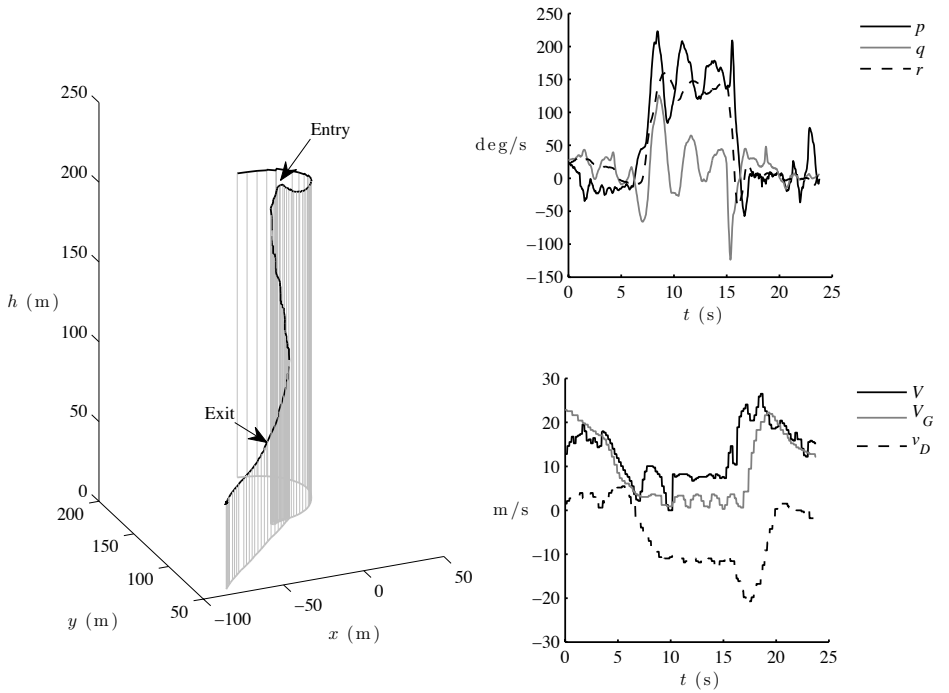


Figure 9. A spin descent.

The trajectory of the orbit (e.g. Fig. 8) was highly dependent on the strength and direction of the wind. In this particular example the wind speed was roughly 7ms^{-1}, resulting in a skewed descent path. The zero wind orbit diameter is estimated at 63·5m, from an average of the lengthwise and widthwise diameters for both orbits. At this radius the deep stall was controllable, other tests involving tighter turn rates made stabilising the aircraft in the turn increasingly difficult.

3.4 Crow braking

Crow braking was achieved by simultaneous deployment of the inboard flaps, to around 45°, and symmetrical upwards deflection of the ailerons. Subsequently roll control was reduced and the rudder was employed for directional control. The symmetric aileron deflection reduces the wing's lift whilst the flaps increase drag. The combined effect of both surface deflections produced a moderate change in the pitching moment, requiring only minor adjustments to the elevator.

Firstly, descents were conducted to determine the effect of the crow-brakes alone. A steady flight path of around −13° was achieved before the crow braking was applied. The vehicle was noticeably slowed after braking, resulting in both a slower airspeed and faster descent.

Next, the braking was combined with a deep stall landing manoeuvre. As before full elevator deflection was used to put the vehicle into deep stall. The combination was found to be highly effective in stabilising the entry into deep stall. Deployment of the outboard ailerons was found to promote a symmetrical stall, reducing pilot workload during entry. Pilot workload was low throughout the descent, and a flight path angle of near −40° was achieved.

https://doi.org/10.1017/S0001924000004292 Published online by Cambridge University Press

3.5 Spin

A spin was entered by reducing the throttle to zero over 5s, followed by a full pitch-up with the elevator, full aileron, and full rudder. Shortly afterwards aileron and rudder deflections were returned to 50% of their travel. The aircraft fell into a near vertical spin descent where the angle-of-attack, exacerbated by the wind, stabilised in the region of 50°. The significant drag resulted in the airspeed dropping by an order of $10ms^{-1}$, resulting in a descent rate of around $11ms^{-1}$. This manifested itself in the typical trajectory of a steep spiral descent visible in Fig. 9, with fast and constant roll and yaw rates of around 180deg/s and 140deg/s respectively. The drop to near-zero ground speed descent speed of about $11ms^{-1}$.

Entry to and exit from the spin required significant control effort, but during the spin itself the control demands were constant. To exit the spin, the control surface inputs were first reduced to zero. Then after a two-second settling time, the throttle was ramped to 90% over 5s. From the point at which the control surfaces were centred the aircraft descended a considerable distance; in one test it dropped approximately 65m before it was able to level off, making this method significantly difficult to moderate should an emergency manoeuvre be required.

4.0 ANALYSIS

From each landing manoeuvre the steady-state flight parameters were obtained from the time history recordings of the flight data, and an average for each manoeuvre type was generated as shown in Table 1.

4.1 Upwash induced angle-of-attack error

The flight path angle, γ, may be computed using Equation (1):

$$\text{Sin}\,\gamma = \text{Cos}\,\alpha\,\text{Cos}\,\beta\,\text{Sin}\,\theta - \text{Sin}\,\beta\,\text{Sin}\,\phi\,\text{Cos}\,\theta - \text{Sin}\,\alpha\,\text{Cos}\,\beta\,\text{Cos}\,\phi\,\text{Cos}\,\theta \quad \ldots (1)$$

where β is the sideslip angle. In the absence of sideslip measurements its effect has been neglected, and its absence in the data is not believed to be significant enough to invalidate the general trends shown. With no sideslip, the flight path angle in Equation (1) simplifies to;

$$\text{Sin}\,\gamma = \text{Cos}\,\alpha\,\text{Sin}\,\theta - \text{Sin}\,\alpha\,\text{Cos}\,\phi\,\text{Cos}\,\theta \quad \ldots (2)$$

In the steady state (denoted with $(\cdot)_e$) the flight path angle may also be obtained geometrically from the trigonometric relations evident from Fig. 10, the most convenient being;

$$-\text{Sin}\gamma_e = \frac{\dot{z}_e}{V_e} \quad \ldots (3)$$

Note that γ is negative below the horizon, hence the negative sign. Substitution into Equation (2) yields an expression that was solved using a simple gradient descent optimisation routine to find α_e. The measured values of steady-state angle-of-attack were used to initialise the search. Alternatively, when the angles of α_e, θ_e, and ϕ_e are small ($\lessapprox 20°$) the approximation;

$$\tilde{\alpha}_e \approx \frac{\dot{z}_e}{V_e} + \theta_e \quad \ldots (4)$$

provides answers with minor increases in error. Either of these methods provides an approximate

https://doi.org/10.1017/S0001924000004292 Published online by Cambridge University Press

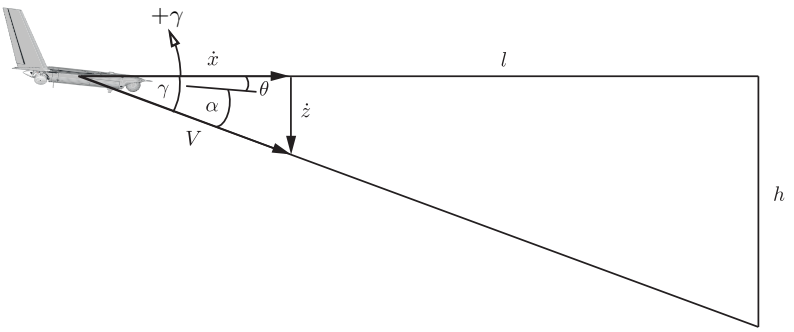


Figure 10. Longitudinal flight path geometry.

estimate for the angle-of-attack, which is denoted by $\tilde{\alpha}_e$. Notably, in doing this it has to be assumed that the other parameters (θ_e, ϕ_e, $\dot{z}_e$, and V_e) have negligible error.

A comparison between the measured (denoted by $\breve{\alpha}_e$) and estimated angle-of-attacks is shown in Fig. 11. The main diagonal line represents the zero error line, whilst the perpendicular distance from each data point to the line is the approximated error in the measurement. 70% of the data points lie above the diagonal indicating the measured result is higher than the estimate. This should be expected since the upwash around the leading edge of the wing will rotate the vane into the local flow and indicate a higher angle-of-attack than expected. The largest deviations from the zero error line can be seen to occur with the deep stall approaches. The overall average error (indicated by the broken line in Fig. 11) was found to be 2·8° with a standard deviation of 4·49°.

4.2 Comparison

The two angle-of-attack parameters $\breve{\alpha}_e$ and $\tilde{\alpha}_e$ give rise to two values for the flight path computed from Equation (1) $\breve{\gamma}_e$ and $\tilde{\gamma}_e$, respectively. Since it was difficult to apply Equation (1) to the spin test logs the glide slope was instead obtained by inspection of the flight trajectory. The result from

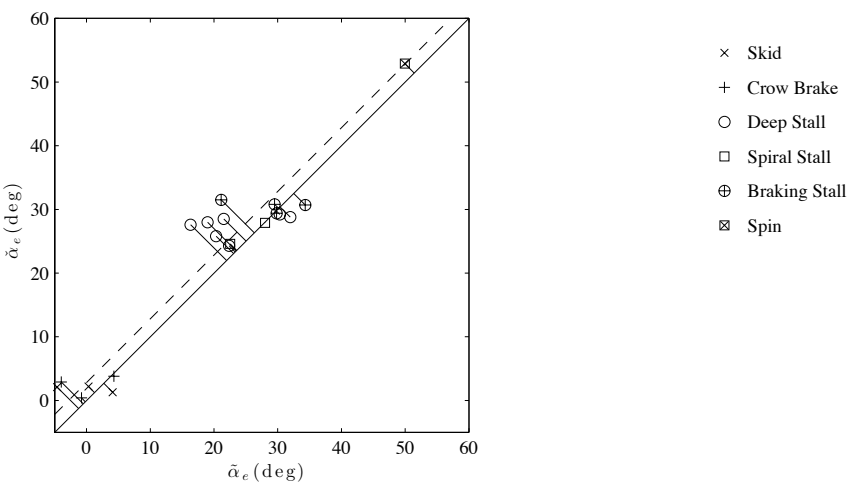


Figure 11. Comparison between estimated (abscissa) and measured (ordinate) angles-of-attack.

https://doi.org/10.1017/S0001924000004292 Published online by Cambridge University Press

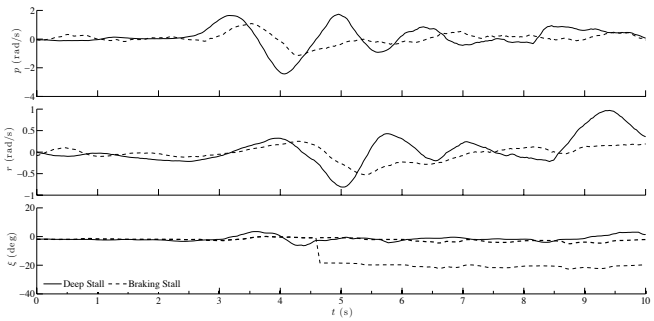


Figure 12. Lateral-directional unsteadiness entering the deep stall. For the braking stall, the aileron controls with the crow brake offset removed is also shown.

Equation (3) provided a similar, but slightly lower value result to that from inspection. For context, the standard glide slope from an instrument landing system for passenger aircraft is three degrees.

The airspeed shown in Table 1 for the spin manoeuvre is estimated from the combined ground and descent speeds, since at such large angles of attack and sideslip the dynamic pressure reading from pitot tubes become unreliable[14,15]; in excess of 40° is reported in Ref. 15. The airspeed measurement during the spin averaged at 7·6ms^{-1} but the ground speed was low (an average of 2·3ms^{-1}), hence the actual airspeed must have been larger given the large descent rate.

The effect of deep stalling is noticeable, where a descent of three times the magnitude of a conventional approach, was possible. The angle-of-attack was an order of magnitude larger than the conventional approach, around 25°. As in Ref. 6 the vehicle quickly became laterally unstable after the dynamic stall due to the unsteady asymmetry in the forces and moments in the immediate post-stall region. The high pilot workload shown between the three and five second mark in Fig. 12 was required to counteract roll and yaw oscillation but once deep stall had been established the corrective action was no longer needed. The control surfaces lose authority due to the flow separation, but it was found that propeller wash enhanced the rudder and elevator authority. A throttle setting of 20% was found to assist with the control without compromising the stall.

In the spiral stall the angle-of-attack was marginally smaller whilst the flight path and airspeed correspondingly larger, though neither by a significant amount. The asymmetric stall across the wing, and subsequent spiral turn contribute to a marginally faster descent than a straight deep stall. Although the ailerons were effective in managing the bank during the spiral, the pilot commented on a notable reduction in their effectiveness. The fact that some control was possible indicates that only the inside wing was stalled, with likely only partial flow separation on the outside – this is the significant difference from the much less controllable spin manoeuvre.

Crow braking on its own can be seen to be effective in reducing the vehicle's airspeed and subsequently allowing a faster decent on a slope approximately 7° steeper. This braking also provides a small, but noticeable, effect when used on the deep stall manoeuvre. The combined deployment of both flaps and ailerons amounts to a variable-span cambered wing. Deploying the ailerons upwards effectively reduces the camber towards the tips, increasing the critical stall angle-of-attack. This offers two benefits: firstly, since stall is mitigated at the wing tip greater control authority is available for transitioning through the unsteady post-stall region to the deep stall. This can be seen in the plot of Fig. 12 – the roll disturbance is delayed and marginal with the crow braking performed, thus requiring less aileron control. Secondly, as the critical angle-of-attack is increased, the aircraft can be pushed into a higher controllable angle-of-attack, enabling a slightly steeper descent gradient at slower speed.

https://doi.org/10.1017/S0001924000004292 Published online by Cambridge University Press

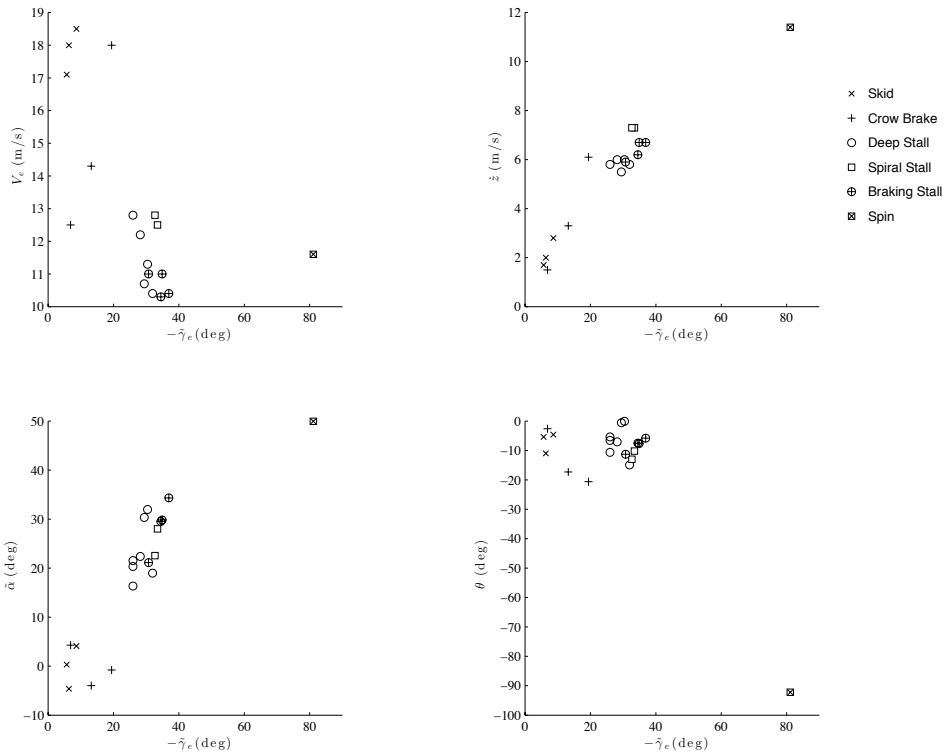


Figure 13. Parameter correlations.

The spin manoeuvres manifested themselves as high angle-of-attack, high-rate descents, with low airspeed. During the spin the SUAV pitch reached −90° and descended at speeds roughly five times larger than that conventional approach, and approximately twice that of the deep stall techniques. The ambient wind was part responsible for a minor drift in the descent. Combined with the vehicle's inertia, this wind was likely responsible for the quite considerable pitching rates visible in Fig. 9. The spin can be seen to be stable, with the damping in all three axes quite noticeable. There was insufficient height however to reach the steady state condition; approximately twice as much time would have been needed.

4.3 Parameter correlation

The order of the landing approaches as listed in Table 1 applies for most of the flight parameters indicating high levels of monotonic correlation between them. This is to be expected from the known kinematic relationship between each.

In Fig. 13 the correlation between the various longitudinal flight parameters and the glide slope angle can be seen. It follows from expectations that at higher glide slopes the descent rate and angle-of-attack increase, whilst the airspeed decreases. The pitch attitude is however less variant and is typically within −20°, the exception being the spin manoeuvre. Figure 14 shows the angle-of-attack data being distinctly grouped by the type of method and demonstrates the inverse relationship with the airspeed, and a somewhat linear relationship with the descent speed.

https://doi.org/10.1017/S0001924000004292 Published online by Cambridge University Press

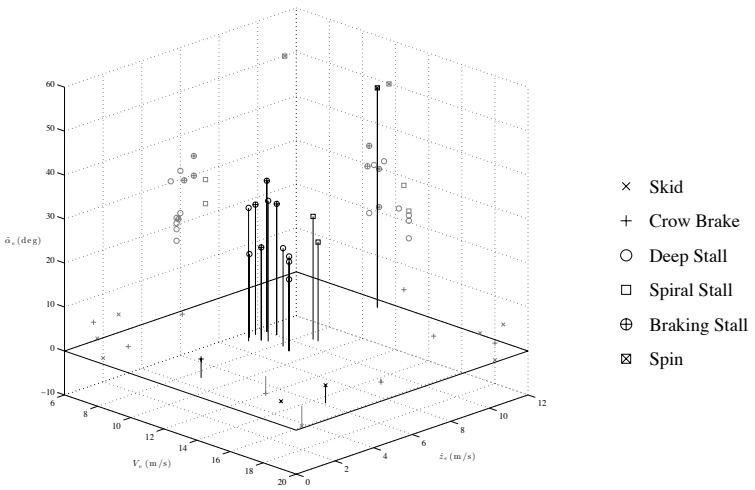
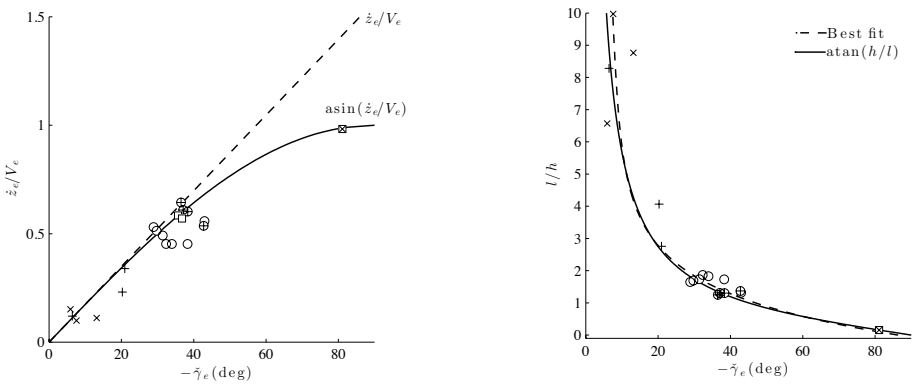


Figure 14. Correlation of airspeed and descent speed with angle-of-attack (estimated). Projections of the data on the rear *V*-α and z-α planes are also shown.



(a) (b)

Figure 15. Correlation of velocity and distance with flight path angle.

It is discernible from these plots that the pilot was able to fly a wide variety of approaches, in terms of the airspeed, pitch angle, descent rate, etc, on the conventional glide slope (including those utilising crow braking). This variation would appear to be constricted when performing the deep stall approaches. It could be said that unfamiliarity with the vehicle in these conditions led to the pilot flying similar behaviours, but is more likely due to the increasing unsteadiness of the flight regime limiting the number of stable equilibrium conditions. It follows that the variety of conditions would continue to be constricted towards the spin manoeuvre, however this cannot be demonstrated with the flight data due to a lack of spin tests.

It follows from Fig. 10 and §4.1 that;

$$-\tilde{\gamma}_e = a\,\mathrm{Sin} = \left(\frac{\dot{z}_e}{V_e}\right) + a\,\mathrm{Tan}\left(\frac{h}{l}\right) \qquad \ldots (5)$$

https://doi.org/10.1017/S0001924000004292 Published online by Cambridge University Press

$$-\tilde{\gamma}_e = \text{aSin}\left(\frac{\dot{z}_e}{V_e}\right) + e_\alpha = a\,\text{Tan}\left(\frac{h}{l}\right) + e_\alpha \qquad \ldots (6)$$

where e_α is a position error in the angle-of-attack measurement Not withstanding these errors the flight data satisfies the relationship reasonably well, as indicated in Fig. 15(a). Some of the results in the region $\breve{\gamma}_e \leq -40°$ also follow the linear approximation $\dot{z}_e/V_e$ reasonably well. The data points for $\tilde{\gamma}_e$ (not shown) appear neatly coincident with the inverse sine function, which is to be expected from the derivation of the parameter. Now the ratio of the distance, l, to height, h, covered in the descent equates to $\dot{x}/\dot{z}$ (Fig. 10). In Fig. 15(b) this 'approach ratio', l/h, is plotted against the computed flight path angle. It is not surprising that the best fit line through the data matches very closely to the geometric model, $-\gamma_e = a\text{Tan}(h/l)$, indicating the overall quality of the data despite the error in the angle-of-attack measurements. Indeed, the line of best fit is near identical to that produced from plotting $\tilde{\gamma}_e$ instead of $\breve{\gamma}_e$. The approach ratio, much like $\dot{z}_e/V_e$, is effectively an indication of the steepness of the descent gradient (and geometrically accurate), as well as an indication of the comparative landing distance required. It is, however, strictly a linear parameter and does not indicate the benefit of the smaller airspace requirements of a spiral or spin descent.

5.0 DISCUSSION

Approach trajectory and velocity, landing accuracy, and airframe and payload robustness are all key considerations when selecting an SUAV approach method. Following the approach, the SUAV must land in a safe manner. Landing techniques currently used on SUAVs in-service include barricades, recovery nets, and interceptor cables[16,17]. Parachute landings are comparatively simpler to implement, however storing the parachute in the airframe, and ensuring successful deployment affects the airframe's design and payload capacity. Due to their reduced complexity drag-only canopies are preferred over parafoil canopies Operating with drag-only canopies requires accurate wind estimation and navigation techniques to predict the optimal deployment position [18], and it is difficult to precisely land the vehicle at the target point under strong wind conditions Unpredictable behaviour under windy conditions can be reduced by deploying the parachute at lower altitudes. Guided parachutes have been able to land vehicles accurately to a specified location[19,20], but at an increase in the complexity of the system and with a potential susceptibility to GPS spoofing. The additional weight and cost of a parachute, along with a supporting guidance, navigation, and control system would limit the size of vehicles it could be installed on; integrating such a system into a SUAV could prove functionally challenging. The landing approach however need not be relegated to a single manoeuvre but instead could be a combination of the most appropriate methods depending on the complexity of the environment, in the manner suggested in Ref. 17.

The deep stall descents allowed for steeper flight path angles which would provide for landing and recovery in more into the deep stall is desirable for controllability and successful development of a steady glide slope. This can be facilitated with larger elevators or by degrading the pitch stiffness through varying the aircraft's inertia. This, and the use of different throttle settings, were not experimentally pursued but briefly investigated. Pilot feedback indicated that a rearward centre of mass promoted easier and more consistent entry to the deep stall, and that a low to medium throttle setting improved controllability. Moderate amounts of throttle provide some propeller wash over the elevator which provides the additional controllability in the stall. Lateral-directional stability is also desirable for controllability in initiating the stall.

Entry into and maintaining the deep stall glide was found to be easier at the lower airspeeds, and the results with the pilot's comments suggest the stability during entry can be enhanced through

https://doi.org/10.1017/S0001924000004292 Published online by Cambridge University Press

the use of crow brakes. Once in the deep stall the vehicle was stable with full elevator and low throttle, with minimal other control inputs required.

The orbiting manoeuvres (spiral deep stall and spin) offer a significant decrease in the recovery space needed. In the case of the spin landing significant altitude must be allowed for to recover from the manoeuvre. Implementing these manoeuvres on SUAVs possessing limited lateral-directional stability and control would therefore be challenging.

The results from this study provide the early work towards implementing these approaches in an automatic fashion on SUAVs. Future work will aim to use the understanding and flight data to develop flight models for each approach manoeuvre for simulation and flight control development. Due to the danger of loss of aircraft from a spin only a small number of spin manoeuvres were carried out, and data from only one manoeuvre was recovered from the logs, which has limited the analysis and understanding for this approach manoeuvre. However the data point appears to agree with expectations and with the overall trends identified in this paper. Future studies will aim to collect more data for the spin manoeuvre to reinforce the results from this work. This will include calibration of the air data instruments to reduce any upwash and position error, especially in the higher angle-of-attack regimes.

6.0 CONCLUSIONS

The results from a series of flight tests of advanced landing approaches show a range of options for landing space and flight paths can be successfully employed on a SUAV. Of the linear approaches, a deep stall landing with crow braking produced the steepest descent gradient of around 35-40° which would significantly reduce landing space requirements. The crow braking component was noticeably effective in stabilising the vehicle as it transitioned through the unsteady post-stall region prior to deep stalling. Wrapping the descent into a spiral profile also gives a further reduction in space requirements, but requires increased control authority. Spin descents require much smaller landing columns and the descent rates attainable are almost five times larger than a conventional glide path landing. However there is a significantly higher risk involved that could be mitigated by transitioning to an alternative mode before landing.

ACKNOWLEDGEMENTS

The authors wish to thank our safety pilot Tom David for his time and expertise. This work was part-funded by DSTL (Defence Science and Technology Laboratory).

REFERENCES

1. Civil Aviation Authority Air Navigation: The Order and the Regulations, CAP 393, August 2012.
2. TANIGUCHI, H. Analysis of Deepstall Landing for UAV, in International Congress of the Aeronautical Sciences, Anchorage, Alaska, USA, 14-19 September 2008.
3. POINTNER, W., KOTSIS, G., LANGTHALER, P. and NADERHIRN, M. Using Formal Methods to Verify Safe Deep Stall Landing of a MAV, in IEEE Digital Avionics Systems Conference, Seattle, Washington, USA, 16-20 October 2011.
4. TAYLOR, R.T. and RAY, E.J. Deep-Stall Aerodynamic Characteristics of T-Tail Aircraft, in NASA Conference on Aircraft Operating Problems, Langley Research Center, Virginia, USA, May 1965.
5. LINA, L.J. and MOUL, M.T. A Simulator Study of T-Tail Aircraft in Deep Stall Conditions, in AIAA/RAeS/JSASS, Aircraft Design and Technology Meeting, Los Angeles, California, USA, November 1965.
6. WHITE, M.D. and COOPER, G.R. Simulator Studies of the Deep Stall, in NASA Conference on Aircraft Operating Problems, Langley Research Center, Virginia, USA, May 1965.

https://doi.org/10.1017/S0001924000004292 Published online by Cambridge University Press

7. WILLIAMS, L.J., JOHNSON JR., J.L. and YIP, L.P. Some Aerodynamic Considerations for Advanced Aircraft Configurations, in AIAA 22nd Aerospace Sciences Meeting, Reno, Nevada, USA, January 1984.
8. EVANGELOU, L.D., SELF, A.W., ALLEN, J.E. and LO, S. Trimmed deep stall on the F-16 Fighting Falcon, *Aeronaut J*, 2001, **105**, (1054), pp 679-683.
9. SIM, A.G. Flight Characteristics of a Manned, Low-Speed, Controlled Deep Stall Vehicle, NASA TM 86041, August 1984.
10. CROWTHER, W.J. Perched Landing and Takeoff for Fixed Wing UAVs, in Symposium on Unmanned Vehicles for Aerial, Ground and Naval Military Operations, Ankara, Turkey, 2000.
11. NAGENDRAN, A., CROWTHER, W.J. and RICHARDSON, R. Biologically inspired legs for UAV perched landing, *IEEE Aerospace and Electronics Magazine*, February 2012, **27**, (2), pp 4-13.
12. RAMAMURTI, R. Computational Fluid Dynamics Study for a Deep Stall AirVehicle, NRL/MR/6410–11-9339, May 2011.
13. SIMONS, M. *Model Aircraft Aerodynamics*, Special Interest Model Books, 4th ed, 1999.
14. FOSTER, J.V. and CUNNINGHAM, K. A GPS-Based Pitot-Static Calibration Method Using Global Output-Error Optimization, in 48th AIAA Aerospace Sciecnes Meeting, Orlando, Florida, USA, January 2010.
15. DIAS, J.N. Flight Path Reconstruction Technqiues Applied to Spin Tests, in AIAA Atmospheric Flight Mechancis Conference, Atlanta, Georgia, USA, June 2014.
16. CROWTHER, W.J. and PRASSAS, K. Post Stall Landing for Field Retrieval of UAVs, in Bristol International. Unmanned Air Vehicle Systems Conference, Bristol, UK, 1999.
17. YOON, S., KIM, H.J. and KIM, Y. Spiral Landing Trajectory and Pursuit Guidance Law Design for Vision-Based Net-Recovery UAV, in AIAA Guidance, Navigation, and Control Conference, Chicago, Illinois, USA, 10-13 August 2008.
18. WYLLIE, T. Parachute recovery for UAV systems, *Aircraft Engineering and Aerospace Technology*, 2001, **73**, (6), pp 542-551.
19. PETRY, G., BEHR, R. and TSCHARNTKE, L. The Parafoil Technology Demonstration (PTD) Project: Lessons Learned.and Future Visions, in 15th CEAS/AIAA Aerodynamic Decelerator.Systems Technology. Conference, Toulouse, France, 8-11 June 1999.
20. STEIN, J.M., MADSEN, C.M. and STRAHAN, A.L. An Overview of the Guided Parafoil System Derived from X-38 Exprience, in 18th AIAA Aerodynamic Decelerator Systems Technology Conference and Seminar, Munich, Germany, 24-26 May 2005.

https://doi.org/10.1017/S0001924000004292 Published online by Cambridge University Press